Experimental Investigation of Pavement Systems Stabilized with Wicking Geotextile-Geogrid Composite over Sensitive Marine Clay Subgrades

Feifan Wang & Mamadou Fall
University of Ottawa, Ottawa, Ontario, Canada

Sam Bhat
Titan Environmental Containment, Ile des Chenes, Manitoba, Canada

ABSTRACT
Sensitive marine clay (SMC), widely distributed in eastern Canada, presents significant challenges for road construction due to its low strength, high compressibility, and poor drainage. This study evaluates the performance of a novel wicking geotextile–geogrid composite for stabilizing pavements constructed over SMC using large-scale physical road model tests under cyclic plate loading. Pavement sections with and without the composite were tested to assess surface settlement, stress distribution, and excess pore-water pressure (EPWP). The reinforced pavement exhibited markedly improved performance, with the load spread angle increasing by approximately 2°, EPWP reduced by 25% (56 to 42 kPa), and accumulated surface settlement reduced by 38.8% after 1,000 loading cycles. These improvements demonstrate the combined benefits of mechanical reinforcement and active drainage provided by the composite, highlighting its potential to enhance the long-term performance and resilience of pavements constructed over weak, high-moisture subgrades.

RÉSUMÉ
L'argile marine sensible (AMS), largement répandue dans l'est du Canada, présente d'importants défis pour la construction routière en raison de sa faible résistance, de sa forte compressibilité et de son faible pouvoir drainant. Cette étude évalue les performances d'un nouveau géosynthétique composite constitué d'un géotextile drainant par capillarité (« *wicking* ») lié à une géogrille, utilisé pour stabiliser des chaussées construites sur des fondations en AMS. L'évaluation repose sur des essais physiques à grande échelle sur modèles routiers soumis à des chargements cycliques par plaque. Des sections de chaussée avec et sans ce composite ont été comparées afin d'évaluer le tassement de surface, la distribution des contraintes et la génération de surpressions interstitielles. Les résultats montrent une amélioration marquée des performances de la chaussée renforcée, avec une augmentation d'environ 2° de l'angle de diffusion des charges, une réduction de 25 % des surpressions interstitielles (56 à 42 kPa) et une diminution de 38,8 % du tassement cumulé en surface après 1 000 cycles de chargement. Ces résultats démontrent les effets combinés du renforcement mécanique et du drainage actif assurés par ce géosynthétique composite, et mettent en évidence son potentiel pour améliorer les performances à long terme et la résilience des chaussées construites sur des sols de fondation faibles à forte teneur en eau.

1 INTRODUCTION

Sensitive marine clay (SMC) is widely distributed in Quebec and Ontario, eastern Canada, where they have formed through a series of post-glacial geological processes. These soils often exhibit soft clay behavior, high sensitivity, and high field water content. Once disturbed, their shear strength can decrease significantly (Taha and Fall, 2014). Such behavior poses significant geotechnical challenges. In the context of road engineering, the use of sensitive marine clay as a subgrade can lead to several issues including uneven surface settlement, pavement cracking, etc. (Tunono and Fall, 2024).

In response to these challenges, geosynthetics have been widely adopted to stabilize weak subgrades. Geosynthetics are polymeric materials, typically manufactured from polypropylene, polyester, polyamide, or polyethylene, and are produced in two- or three-dimensional structures (Puppala et al., 2020). They serve multiple functions, including reinforcement, filtration, separation, and drainage, thereby improving the performance of subgrade soils. Common types of geosynthetics include geotextiles, geogrids, geonets, geomembranes, geosynthetic clay liners, prefabricated vertical drains, geocomposites, geocells, and geofoam. Among these, geogrids and geotextiles are most commonly used for subgrade stabilization due to their effectiveness in providing mechanical reinforcement and facilitating drainage.

Numerous studies have been conducted to investigate the stabilization mechanisms and performance of geogrids and geotextiles in road engineering. Christopher (2016) identified three primary reinforcement mechanisms provided by geosynthetics: (1) lateral restraint, achieved through improved shear resistance at the soil–geosynthetic interface; (2) increased bearing capacity, resulting from the redirection of potential failure surfaces into zones of higher shear strength; and (3) membrane support, which

distributes applied loads and enhances load transfer. Gu et al. (2016) showed that geogrids reduce compressive stress and strain in the base and subgrade but have little effect on tensile strain in the asphalt layer, indicating improvement in rutting resistance rather than fatigue life. Praveen and Baadiga (2026) demonstrated that increasing subgrade California bearing ratio, CBR (6%–15%) reduces the incremental benefits of geogrid reinforcement for a constant base thickness. This trend indicates a transition in geogrid function, from active deformation control in weak subgrades to a more limited role in load distribution under stiffer conditions. Regarding the wicking geotextile-geogrid composite, Liu et al. (2025a, 2025b) reported that wicking grids achieve significantly faster and farther moisture migration than woven wicking geotextiles, resulting in an approximately 58% improvement in bearing capacity compared to non-wicking grids.

While geosynthetic research has progressed in recent years, understanding of wicking grid systems remains limited. In particular, their behavior and effectiveness in highly compressible, sensitive marine clay subgrades have not yet been systematically investigated.

The objective of this study is to investigate the performance of wicking geotextile – geogrid composites in pavements over highly saturated marine clay using an integrated experimental approach. Specifically, large-scale cyclic plate loading tests are conducted to (i) evaluate stabilization effects and (ii) monitor excess pore water pressure and permanent settlement.

2 EXPERIMENTS AND METHODOLOGY

Two test sections were considered in this study: a control section and a reinforced section. The physical models comprised an asphalt concrete (AC) layer, an unbound base course, and a subgrade. No WickGrid™ was installed in the control section, whereas the WickGrid™ was placed at the base course–subgrade interface in the reinforced section.

2.1 Materials

The SMC used for subgrade was collected at South Gloucester, Ottawa, Canada. The soil used in this study is a marine clay with a water content of 82%, a clay fraction of 84%, a natural void ratio of 2, and a sensitivity of 6. The liquid limit and plastic limit were determined to be 66.7% and 26.5%, respectively. Compaction characteristics were evaluated using the standard proctor test in accordance with ASTM D698, which indicated an optimum moisture content of 22% (Figure 1). Figure 2 shows the particle size distribution for used SMC (Leda clay).

Granular A was used for the base course. Compaction properties were obtained from the standard proctor test in accordance with ASTM D698, obtaining a maximum dry density of 2.2 g/cm³ and an optimum moisture content of 6% (Figure 1). The particle size distribution is shown in Figure 2.

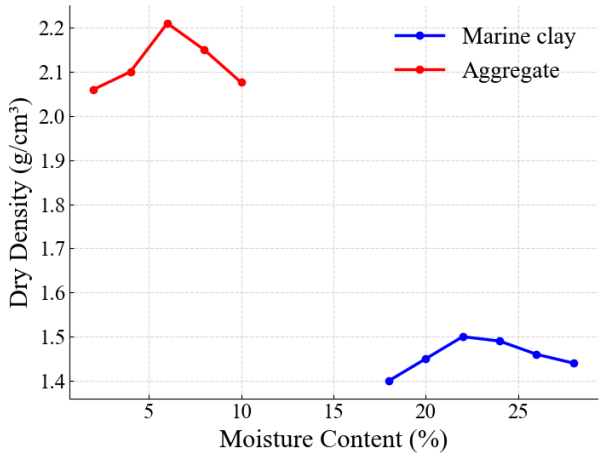


Figure 1. Results of standard proctor tests for used SMC and aggregate.

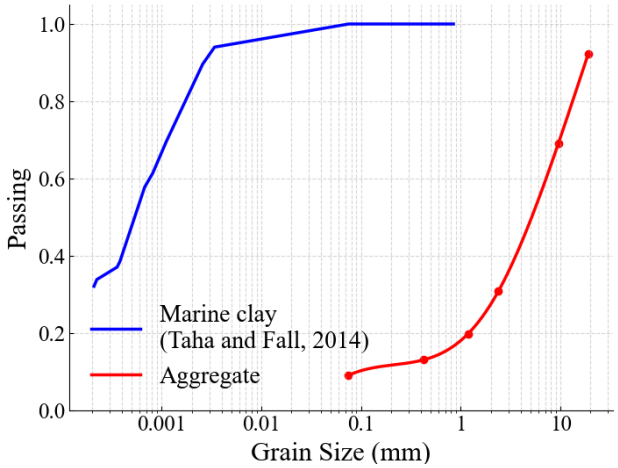


Figure 2. Particle size distribution of the used SMC and aggregate.

A weak subgrade was reproduced by preparing the SMC at an initial water content of 40%, representing conditions of low matric suction and diminished effective stress. This state yielded a California bearing ratio (CBR) below 3%, consistent with commonly accepted thresholds for weak subgrades. Previous work by Pokharel (2010) established a relationship between CBR and the undrained shear strength of fine-grained soils shown as Equation 1:

$$CBR = \frac{c_u}{20.5} \quad [1]$$

where c_u is undrained shear strength in kPa. Accordingly, vane shear tests were conducted across a range of moisture contents to quantify the undrained strength. For the specimen at 40% water content, the measured undrained shear strength corresponds to a CBR of less than 3%, confirming that the target weak subgrade condition was achieved.

The AC layer in this study was constructed using a commercially available reactive cold-mix asphalt (CMA). The aggregates satisfy relevant AASHTO T-85 and ASTM

C127 requirements, with a specific gravity ≤ 3.000, sand equivalent > 80, and fine aggregate angularity > 45. Table 1 shows the gradation analysis of the CMA.

Table 1. The particle size distribution of the used cold-mix asphalt (CMA).

Sieve sizes	Passing (%)
1/2" sieve	100
3/8" sieve	100
#4 sieve	85 ~ 100
#8 sieve	20 ~ 55
#16 sieve	12 ~ 32
#200 sieve	3 ~ 6

The geosynthetic used in this study is a wicking grid manufactured by Titan Environmental Ltd. It consists of a biaxial geogrid integrated with a nonwoven wicking geotextile. The key properties are summarized in Table 2.

Table 2. The properties of used geosynthetics.

Geosynthetic	Property	Value	
		MD	CD
Biaxial geogrid	Radial stiffness @ 0.5% strain (kN/m)	550.0	550.0
	Secant stiffness EA @ 2% strain (kN/m)	700.0	700.0
	Junction efficiency (%)	>95	>95
	Flexural rigidity (mg-cm)	2000000	
	Aperture stability (kg-cm/deg)	11.0	
	Minimum rib thickness (mm)	2.5	1.5
	Aperture size (mm)	38.0	38.0
Non-woven wicking geotextile	Grab strength (N)	935	
	Trapezoidal tear (N)	427	
	CBR puncture strength (kN)	2.6	
	Permittivity (sec^{-1})	1.52	
	Flow rate (L/min/m²)	4530	
	Apparent opening size (mm)	0.075	
	Mass per unit area (g/m²)	235	

[1]MD refers to the in-plane direction parallel to manufacture, while CD denotes the perpendicular direction. (Data supplied by Titan Environmental Containment Ltd. 2024)

2.2 Experiment Setup

A large-scale plate loading system (1.0 m × 1.0 m × 1.4 m) was used to evaluate two pavement scenarios: an unreinforced case (control section) and a section incorporating WickGrid™ at the base–subgrade interface (reinforced section). The pavement profile included a 600 mm subgrade layer overlain by a 250 mm base and a 50 mm asphalt layer. Experimental layout and material details are provided in Figure 3 and Table 3.

Instrumentation was arranged to capture hydraulic and mechanical responses. Moisture content, pore-water pressure, and soil stress were measured at the base course-subgrade interface using EC-5 sensors, HC-25 transducers, and HC-16 cells, respectively. The surface deformation was monitored using LVDTs positioned at offsets of 150 mm from the load center.

Prior to placement, the SMC was remolded by air-drying and crushing to a particle size smaller than 2 mm to ensure repeatability. Water was then added to reach a target moisture content of 40%, representing weak subgrade conditions, and the mixture was sealed and conditioned overnight for uniform moisture distribution. The aggregate was similarly prepared at its optimum moisture content (6%) and conditioned prior to compaction. Random sampling before placement confirmed average moisture contents of approximately 40% for the clay and 6% for the aggregate.

The pavement layers were constructed sequentially in the test box. The subgrade and base course were placed in lifts and compacted to a target relative density of 90%, with the WickGrid™ installed at the subgrade surface before base placement. The AC layer was then placed in two lifts and compacted to the designed thickness, with a bonding coat applied to improve interlayer interaction. After construction, the system was allowed to drain for 24 h prior to testing.

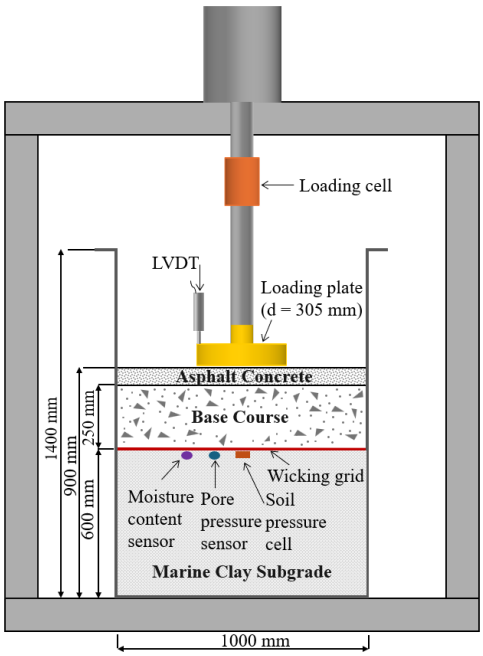


Figure 3. The setup for plate loading test.

Table 3. The information for tested pavement.

Layer	Thickness	Material	Properties
AC layer	50 mm	CMA	water-reactive material
Base course	250 mm	granular A	Water content: 6% Compaction degree: >90%
Subgrade	600 mm	SMC	Water content: 40% Compaction degree: >90% CBR = 2.2%

[2]no geosynthetic was placed in the control group.

Cyclic loading was applied through a rigid steel plate with a diameter of 300 mm to simulate tire loading. Each test consisted of 1,000 loading cycles, which, according to geotechnical shakedown theory and previous large-scale

experimental studies (e.g., Guo et al., 2021), are sufficient to capture the long-term mechanical response of pavement systems. The loading scheme is shown in Figure 4. A peak load of 40 kN was applied, representing a single-wheel load corresponding to half of an 80 kN axle, with an associated contact pressure of 550 kPa. The loading frequency was 0.77 Hz. In each cycle, the load increased linearly from 0.5 kN to 40 kN over 0.3 s, was held for 0.2 s, and then decreased back to 0.5 kN, followed by a 0.5 s rest period before the next cycle.

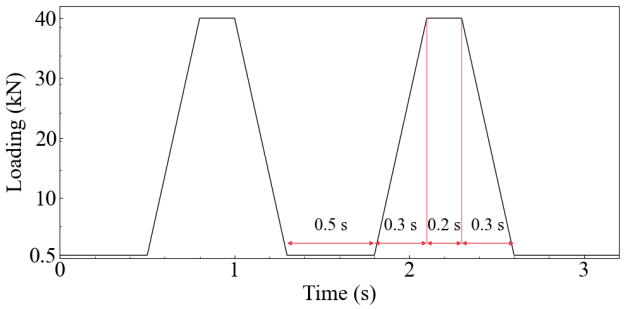


Figure 4. The applied loading.

3 RESULTS

In this section, the evolution of surface permanent settlement, maximum vertical stress, and excess pore water pressure (EPWP) with loading cycles are presented for both the control and reinforced sections at the base course–subgrade interface to evaluate the stabilization effect of the WickGrid™.

3.1 Surface Settlement

The maximum surface plastic settlement was measured using the LVDT 150 mm away from the loading center. The results for control section and reinforced section are shown in Figure 5.

After 1000 loading cycles, the permanent surface settlement at the loading center reached 92.3 mm in the control section and 56.2 mm in the WickGrid™-reinforced section, corresponding to a reduction of approximately 39% due to the presence of WickGrid™. The reduced final settlement in the reinforced case confirms the stabilization benefit of WickGrid™. For both sections, settlement accumulated rapidly during the early stage of loading, particularly within the first 100 cycles, and the rate gradually declined with further cycling, indicating progressive strain hardening of the pavement system under the current loading condition. Sun et al. (2015) observed that under higher loading amplitudes, soils exhibited strain-softening behavior, with plastic strain accumulating at an increasing rate once the applied stress exceeded the bearing capacity. In contrast, the decreasing settlement rate observed in the present study suggests that the applied load remained below the critical applied loading of both test sections.

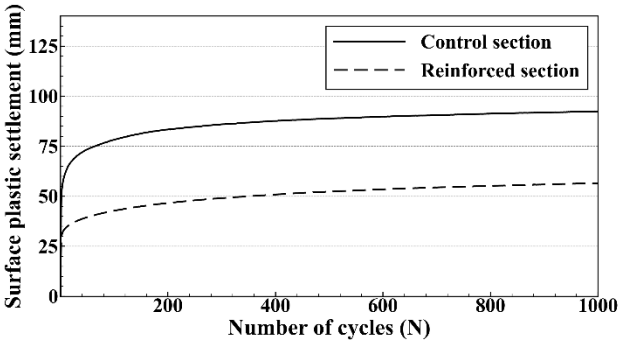


Figure 5. Maximum surface settlement under 1000 loading cycles.

To evaluate the reinforcement performance of the geosynthetic, the settlement reduction factor (SRF) was adopted as an index, as defined in Equation 2:

$$SRF = (S_{control}/S_{reinforced}) \quad [2]$$

where $S_{control}$ represents the total surface settlement of the unreinforced pavement section, whereas $S_{reinforced}$ denotes the corresponding settlement of the WickGrid™-reinforced section. The calculated SRF at the loading center was 1.64, corresponding to a settlement reduction of 39%.

3.2 Vertical Stress

The earth pressure cell was placed at the base course-subgrade interface to monitor the vertical stress during loading cycles.

Figure 6 shows the maximum vertical stress with loading cycles. In both sections, the maximum vertical stress rose rapidly during the initial loading stage, then gradually decreased and eventually stabilized. This early increase is mainly attributed to material densification and structural rearrangement under repeated loading. However, such a trend was not observed at the base course–subgrade interface in the reinforced section, which may be related to initial instability during the early cycles.

At the base course–subgrade interface, the stabilized maximum vertical stress was 140 kPa in the reinforced section, compared with 160 kPa in the control section. This reduction can be attributed to the lateral confinement provided by the WickGrid™ through mechanical interlocking with the aggregate base. Such confinement enhances base stiffness and improves stress distribution, thereby decreasing the vertical stress transferred to the subgrade.

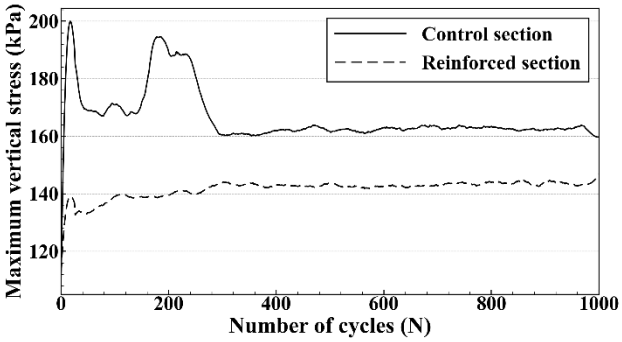


Figure 6. Vertical stress development under cyclic loading (1000 cycles) at the base course–subgrade interface.

Load transfer efficiency was quantified by the load spread angle (LSA), a parameter describing stress dispersion within the pavement structure, as given in Equation 3 based on Thakur et al. (2012):

$$P_i = \frac{P}{\pi[r_{LSA}+h_{LSA}\,tan(\alpha_{LSA})]^2} \quad [3]$$

where P_i represents the vertical stress measured at the loading center of the base course–subgrade interface, P is the applied load, r_{LSA} is the radius of the loading plate, h_{LSA} is the base course thickness, and α_{LSA} denotes the stress distribution angle relative to the vertical direction. A greater LSA value indicates more effective stress dispersion within the pavement system and consequently lower vertical stress within the subgrade.

Figure 7 shows the variation of LSA with loading cycles for both sections. The stabilized values were 23° for the control section and 26° for the WickGrid™-reinforced section. In both cases, LSA initially decreased with repeated loading, followed by partial recovery and eventual stabilization. This response indicates that early deformation in the base course caused stress transfer to become more localized, increasing vertical stress concentration beneath the loading area.

Throughout the test, the reinforced section maintained a higher LSA than the control section, reflecting improved load dispersion and lower stress concentration at the base–subgrade interface. At the beginning of loading, the difference between the two sections was limited (23.6° for the control and 24.5° for the reinforced section). A clear transition occurred within the first 300 cycles, during which LSA dropped more significantly in the control section, while the reinforced section showed a gradually reduced rate of change. After this stage, the reinforced section remained relatively stable, suggesting that the load-spreading function of WickGrid™ developed progressively as tensile strains were mobilized within the geosynthetic.

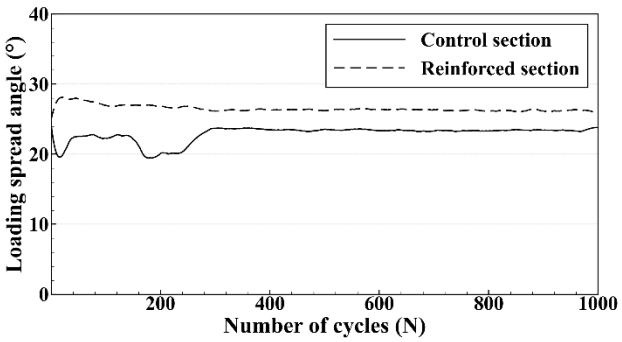


Figure 7. Development of load distribution angle under 1000 loading cycles at the base course–subgrade interface.

3.3 Excess Pore Water Pressure

The pore water pressure was measured using the pore pressure sensor at the base course-subgrade interface. Figure 8 shows the EPWP with 1000 loading cycles.

At the base course–subgrade interface, EPWP in both sections rose rapidly during the initial loading stage, mainly due to the significant early deformation of the pavement structure (Figure 5). With continued cyclic loading, EPWP gradually dissipated, showing a trend similar to that reported by Hu et al. (2023).

A sharper EPWP reduction was observed in the control section within the first 50 cycles. This may be related to its higher water content after the one-day drainage period, which increased permeability and promoted pore water migration from zones of high pressure, resulting in faster pressure dissipation.

During the steady-state stage, the EPWP at the base–subgrade interface remained around 56 kPa in the unreinforced section, whereas only 42 kPa was recorded in the reinforced section. The EPWP reduction was approximate 25% reduction. In addition, after completion of the tests, when the soil was removed from the loading box, significant water accumulation was clearly observed at the bottom of the base course. The lower pore pressure level indicates that WickGrid™ improved drainage conditions and suppressed the accumulation of excess pore water pressure under repeated loading.

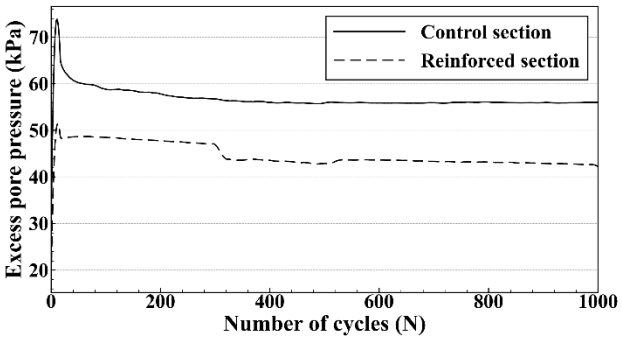


Figure 8. Development of excess pore water pressure (EPWP) under 1000 loading cycles at the base course–subgrade interface.

4 ENGINEERING IMPLICATIONS

The WickGrid™ composite geosynthetic installed at the base course–subgrade interface provides both mechanical and hydraulic functions. The biaxial geogrid contributes to lateral confinement through interaction with the aggregate, which improves load distribution and reduces stress concentration. Furthermore, the non-woven wicking geotextile forms a horizontal drainage layer that facilitates moisture redistribution, even under low hydraulic gradients. This drainage condition reduces the accumulation of water at the base of the granular layer and limits the build-up of excess pore water pressure under cyclic loading. As a result, the stabilized EPWP at the interface decreases from 56 kPa in the control section to 42 kPa in the reinforced section. The corresponding reduction in pore water pressure contributes to an increase in effective stress in the subgrade.

The combined effects of mechanical confinement and drainage lead to improved overall performance, including reduced settlement and lower pore water pressure, indicating enhanced stability of the pavement system under coupled hydro-mechanical conditions, especially for the pavement structures with high water content weak subgrade.

5 CONCLUSION

Large-scale cyclic plate loading tests were conducted to evaluate the performance of pavement systems stabilized with a wicking geotextile–geogrid composite (WickGrid™) over SMC subgrades. The results show that WickGrid™ significantly improved pavement performance under repeated loading.

The reinforced section exhibited lower permanent surface settlement, with the final settlement reduced by 39% compared with the control section. Vertical stress at the base course–subgrade interface also decreased, while the load spread angle increased, indicating improved stress distribution and reduced stress concentration in the weak subgrade.

The stabilized EPWP decreased from 56 kPa in the control section to 42 kPa in the reinforced section, demonstrating faster drainage and reduced pore pressure build-up. These improvements could be attributed to the combined action of the high-stiffness geogrid providing lateral confinement and the wicking geotextile promoting horizontal drainage and moisture redistribution.

These results provide improved understanding of the coupled reinforcement–drainage mechanism of WickGrid™ and demonstrate its effectiveness for stabilizing pavements over high-moisture weak subgrades. The findings also highlight its potential to support more sustainable and resilient road infrastructure in sensitive marine clay regions such as Quebec and Ontario.

ACKNOWLEDGMENTS

The authors sincerely thank the University of Ottawa, Titan Environmental Containment Ltd. for their financial, technical support and the supply of the material and the Natural Sciences and Engineering Research Council of Canada (NSERC) for their financial and administrative support for this project.

REFERENCES

Christopher, B.R. 2016. *Geotextiles used in reinforcing paved and unpaved roads and railroads*, Elsevier eBooks, pp. 305–335. https://doi.org/10.1016/b978-0-08-100221-6.00014-0.

Gu, F., Luo, X., Luo, R., Lytton, R.L., Hajj, E.Y., and Siddharthan, R.V. 2016. Numerical modeling of geogrid-reinforced flexible pavement and corresponding validation using large-scale tank test, *Construction and Building Materials*, 122, pp. 214–230. https://doi.org/10.1016/j.conbuildmat.2016.06.081.

Guo, J., Han, J., Zhang, X. and Li, Z. 2021. Experimental evaluation of wicking geotextile-stabilized aggregate bases over subgrade under rainfall simulation and cyclic loading, *Geotextiles and Geomembranes*, 49(6), pp. 1550–1564. https://doi.org/10.1016/j.geotexmem.2021.07.00.

Hu, J., Zhang, H., Li, Z., Yang, S., Zhang, S., Li, H., and Lu, M. 2023. Study on pore-water pressure variation and deformation characteristics of warm frozen soils under confined dynamic loading, *Cold Regions Science and Technology*, 214, p. 103968. https://doi.org/10.1016/j.coldregions.2023.103968.

Liu, M., Liu, J., Bhat, S., Gupta, R., and Lin, C. 2025a. Evaluation of water removal capability of wicking nonwoven geotextiles, *Geotextiles and Geomembranes*, 53(6), pp. 1228–1241. https://doi.org/10.1016/j.geotexmem.2025.06.001.

Liu, M., Liu, J., Bhat, S., Gao, Y., and Lin, C. 2025b. Model tests on wicking geosynthetic composite reinforced bases over weak subgrade, *Geotextiles and Geomembranes*, 53(4), pp. 938–949. https://doi.org/10.1016/j.geotexmem.2025.03.006.

Pokharel, S.K. 2010. Experimental study on geocell-reinforced bases under static and dynamic loading. Ph.D. thesis, Department of Civil, Environmental and Architectural Engineering, University of Kansas, Lawrence, KS, USA.

Puppala, A.J., Banerjee, A. and Congress, S.S.C. 2020. *Geosynthetics in geo-infrastructure applications*, Elsevier eBooks, pp. 289–312. https://doi.org/10.1016/b978-0-12-818260-4.00007-7.

Praveen, B.S. and Baadiga, R. 2026. Full-scale field studies on performance evaluation of geogrid reinforced flexible pavements through cyclic plate load tests, *Geotextiles and Geomembranes*, 54(4), pp. 668–678. https://doi.org/10.1016/j.geotexmem.2026.03.004.

Sun, X., Han, J., Kwon, J., Parsons, R.L., and Wayne, M.H. 2015. Radial stresses and resilient deformations of geogrid-stabilized unpaved roads under cyclic plate loading tests, *Geotextiles and Geomembranes*, 43(5), pp. 440–449. https://doi.org/10.1016/j.geotexmem.2015.04.018.

Taha, A. and Fall, M. 2014. Shear behavior of sensitive marine clay–steel interfaces, *Acta Geotechnica*, 9(6), pp. 969–980. https://doi.org/10.1007/s11440-014-0321-4.

Thakur, J.K., Han, J., Pokharel, S.K., and Parsons, R.L. 2012. Performance of geocell-reinforced recycled asphalt pavement (RAP) bases over weak subgrade under cyclic plate loading, *Geotextiles and Geomembranes*, 35, pp. 14–24. https://doi.org/10.1016/j.geotexmem.2012.06.004.

Tunono, C., and Fall, M. 2024. Column experiments to study the thermo-hydro-mechanical-chemical behavior of sensitive marine clay subgrade soil treated with lime, *Bulletin of Engineering Geology and the Environment,* 83(4):120.